

POSTBUCKLING ANALYSIS OF CENTRALLY COMPRESSED BARS WITH OPEN THIN-WALLED CROSS SECTION

UDC 539.4(045)=20

G. I. Ioannidis

National Technical University of Athens, 42 Patission Str., Athens, Greece

Abstract. *In this paper the postbuckling behaviour of simply supported bars with uniform open thin walled cross sections, subjected to a centrally applied compressive load is examined. The analysis refers to sections for which the centroid does not coincide with the shear centre; hence the bars lose their stability through simultaneous bending and torsion. The postbuckling equilibrium paths are established using a simple analytic technique leading to the conclusion that the margins of postbuckling strength are rather limited. Attention is also focused in the first yielding, in case of bars made of ideal elastic – ideal plastic material, occurring at the initial part of the post-critical path and associated with the maximum combined normal stress due to axial compression, bending and warping. Numerical examples are also presented for various types of cross-sections.*

Key words: *postbuckling behaviour of simply supported bars, open thin walled cross sections, shear centre, centroid, stability, post-critical path, ideal elastic, ideal plastic material.*

1. INTRODUCTION

The use of light-weight and stiff structures is steadily increasing in modern structural design. Thus, thin walled (closed or open) cross sections are extensively used in various engineering applications. However, the design of structures composed from thin-walled cross-sections poses particular problems in their analysis, which become more severe in the case of asymmetric cross-sections, whose centroid does not coincide with the shear centre.

Instability problems of thin-walled sections have been the subject of extensive research. An excellent reference is the early classical work presented by Vlassov [1]. Reviewing the present state of the art one could refer to the books presented by Chen and Atsuta [2] and Trahair [3], in addition to a large number of papers based on linear analyses. Moreover, studies concerning the postbuckling behaviour of beams and beam-columns under transverse loading have been presented by several authors [4-7].

Equating the internal and the corresponding external bending and torsional moments at an arbitrary point of axis z , the system of differential equations of equilibrium, in the case of a pin-ended bar, can be written as follows [11]:

$$\begin{aligned} EI_y \frac{d^2 u}{dz^2} + Pu &= -Py_o \phi \\ EI_x \frac{d^2 v}{dz^2} + Pv &= -Px_o \phi \\ EC_w \frac{d^3 \phi}{dz^3} - \left(GJ - \frac{I_o}{A} P \right) \frac{d\phi}{dz} &= Px_o \frac{dv}{dz} - Py_o \frac{du}{dz} \end{aligned} \quad (1)$$

where EI_x and EI_y are the bending rigidities about the principal centroidal axes x and y , GJ and EC_w the torsional rigidity and the warping rigidity of the cross-section respectively and $I_o = I_x + I_y + (x_o^2 + y_o^2)A$, A being the cross-sectional area.

Combining eqs (1) one can obtain the following differential equation with respect to ϕ which governs the elastic instability of the bar due to a combination of bending and torsion

$$EC_w \phi''' - \left(GJ - \frac{I_o}{A} P \right) \phi'' - P * (k_x^2 x_o^2 + k_y^2 y_o^2) \phi = Pk_y^2 y_o u - Pk_x^2 x_o v \quad (2)$$

where the prime denotes differentiation with respect to z and

$$k_x^2 = P/EI_x, \quad k_y^2 = P/EI_y. \quad (3)$$

Using the shape functions

$$u = u_o \sin \frac{\pi z}{\ell}, \quad v = v_o \sin \frac{\pi z}{\ell}, \quad \phi = \phi_o \sin \frac{\pi z}{\ell} \quad (4)$$

(where v_o , u_o , ϕ_o are the lateral deflections and the angle of rotation at the middle of the bar, respectively) which satisfy the boundary conditions

$$\begin{aligned} u(0) = v(0) = \phi(0) = 0, \quad u(\ell) = v(\ell) = \phi(\ell) = 0 \\ \frac{d^2 u(0)}{dz^2} = \frac{d^2 v(0)}{dz^2} = \frac{d^2 \phi(0)}{dz^2} = 0, \quad \frac{d^2 u(\ell)}{dz^2} = \frac{d^2 v(\ell)}{dz^2} = \frac{d^2 \phi(\ell)}{dz^2} = 0, \end{aligned} \quad (5)$$

one can obtain, for a non trivial solution, the following instability equation [7]

$$\begin{vmatrix} P - P_y & 0 & Py_o \\ 0 & P - P_x & -Px_o \\ Py_o & -Px_o & \frac{I_o}{A} (P - P_t) \end{vmatrix} = 0 \quad (6)$$

where

$$P_x = \frac{\pi^2 EI_x}{\ell^2}, P_y = \frac{\pi^2 EI_y}{\ell^2}, P_t = \frac{A}{I_o} \left(GJ - \frac{\pi^2}{\ell^2} EC_w \right)$$

denote the critical loads of flexural buckling about the x and y axes and the critical load of torsional buckling respectively. Clearly, the smallest value of P, obtained from equation (6), is the critical instability load for the case in which instability occurs via combined bending and torsion. It can be shown [11] that eq. (6) has three positive roots, the smallest of which (critical load) is smaller than P_x , P_y and P_t .

3. NON LINEAR - POSTBUCKLING ANALYSIS

This section deals with the discussion of the nature of the critical state and the establishment of the initial part of the postbuckling equilibrium path. To this end a more accurate relationship for the curvature is used due to which the first and the second of eqs. (1) can be written as follows [6]:

$$\begin{aligned} P(u - y_o \phi) &= EI_y \frac{u''}{(1-u'^2)^{1/2}} \\ P(v - x_o \phi) &= EI_x \frac{v''}{(1-v'^2)^{1/2}} \end{aligned} \quad (8)$$

Using the approximations

$$\frac{u''}{(1-u'^2)^{1/2}} = u'' \left(1 + \frac{1}{2} u'^2 \right) \text{ and } \frac{v''}{(1-v'^2)^{1/2}} = v'' \left(1 + \frac{1}{2} v'^2 \right)$$

eqs.(8) can be written

$$\begin{aligned} u'' + k^2 u &= -k_y^2 y_o \phi - \frac{1}{2} u'' u'^2 \\ v'' + k^2 v &= -k_x^2 x_o \phi - \frac{1}{2} v'' v'^2 \end{aligned} \quad (9)$$

Following the approximate analytic technique developed by Kounadis [9,10] for solving non linear boundary-value problems the arbitrary (but satisfying the boundary conditions) functions (4) are introduced in the second term of eqs. (9) which can be expressed as

$$\begin{aligned} u'' + k_y^2 u &= -k_y^2 y_o \phi \sin \pi \xi + \frac{u_o \pi^4}{2} \cos^2 \pi \xi \cdot \sin \pi \xi \\ v'' + k_x^2 v &= -k_x^2 x_o \phi \sin \pi \xi + \frac{v_o \pi^4}{2} \cos^2 \pi \xi \cdot \sin \pi \xi \end{aligned} \quad (10)$$

where

$$\begin{aligned}\bar{\xi} &= z/\ell, \quad \bar{\mathbf{u}} = \mathbf{u}/\ell, \quad \bar{\mathbf{v}} = \mathbf{v}/\ell, \quad \bar{y}_o = y_o/\ell, \quad \bar{x}_o = x_o/\ell \\ \bar{k}_y &= k_y^2 \ell^2, \quad \bar{k}_x = k_x^2 \ell^2, \quad \bar{\mathbf{u}}_o = \mathbf{u}_o/\ell, \quad \bar{\mathbf{v}}_o = \mathbf{v}_o/\ell\end{aligned}\quad (11)$$

Taking into account the boundary conditions

$$\bar{\mathbf{u}}(0) = \bar{\mathbf{v}}(0) = \bar{\mathbf{u}}(1) = \bar{\mathbf{v}}(1) = 0 \quad (12)$$

the integrals of eqs. (10) are

$$\begin{aligned}\bar{\mathbf{u}}(\xi) &= \left[\frac{\bar{k}_y \bar{y}_o \bar{\phi}_o - (\pi^4/8) \bar{\mathbf{u}}_o}{\bar{k}_y - \pi^2} \right] \sin \pi \xi + \frac{(\pi^4/8) \bar{\mathbf{u}}_o}{\left(\bar{k}_y - 9\pi^2 \right)} \sin 3\pi \xi, \quad \left(\bar{k}_y \neq \pi^2, 9\pi^2 \right) \\ \bar{\mathbf{v}}(\xi) &= \left[\frac{\bar{k}_x \bar{x}_o \bar{\phi}_o - (\pi^4/8) \bar{\mathbf{v}}_o}{\bar{k}_x - \pi^2} \right] \sin \pi \xi + \frac{(\pi^4/8) \bar{\mathbf{v}}_o}{\left(\bar{k}_x - 9\pi^2 \right)} \sin 3\pi \xi, \quad \left(\bar{k}_x \neq \pi^2, 9\pi^2 \right)\end{aligned}\quad (13)$$

Integrating once the third of eqs. (1) and setting into the second term the expressions of $\bar{\mathbf{v}}(\xi)$, $\bar{\mathbf{u}}(\xi)$ from eqs. (13) one can take

$$\phi''(\xi) + k_t \phi(\xi) = \beta^2 \left[\left(A_1 \bar{y}_o + A_2 \bar{x}_o \right) \sin \pi \xi + \left(A_4 \bar{x}_o - A_3 \bar{y}_o \right) \sin 3\pi \xi \right] \quad (14)$$

where

$$k_t = k_t^2 \ell^2, \quad k_t^2 = \left[\frac{I_o}{A} P - GJ \right] / EC_w, \quad \beta^2 = P \ell^4 / EC_w$$

and

$$\begin{aligned}A_1 &= \frac{\bar{k}_y \bar{y}_o \bar{\phi}_o - (\pi^4/8) \bar{\mathbf{u}}_o}{\bar{k}_y - \pi^2}, & A_2 &= \frac{\bar{k}_x \bar{x}_o \bar{\phi}_o - (\pi^4/8) \bar{\mathbf{v}}_o}{\bar{k}_x - \pi^2} \\ A_3 &= \frac{(\pi^4/8) \bar{\mathbf{u}}_o}{\left(\bar{k}_y - 9\pi^2 \right)}, & A_4 &= \frac{(\pi^4/8) \bar{\mathbf{v}}_o}{\left(\bar{k}_x - 9\pi^2 \right)}\end{aligned}\quad (15)$$

From eq. (14), with the aid of the boundary conditions $\phi(0)=\phi(1)=0$, results the following function for the angle of rotation

$$\phi(\xi) = \beta^2 \left[\left(\frac{A_1 \bar{y}_o + A_2 \bar{x}_o}{\bar{k}_t - \pi^2} \right) \sin \pi \xi + \left(\frac{A_4 \bar{x}_o + A_3 \bar{y}_o}{\bar{k}_t - 9\pi^2} \right) \sin 3\pi \xi \right] \quad (16)$$

The application of eqs. (13) and (16) for $\xi = 0.5$ results in the following system of equations

$$\begin{aligned} \bar{u}_o(k_y - \pi^2)(k_y - 9\pi^2) &= -\bar{k}_y \bar{y}_o \phi_o(k_y - 9\pi^2) - \pi^6 \bar{u}_o \\ \bar{v}_o(k_x - \pi^2)(k_x - 9\pi^2) &= -\bar{k}_x \bar{x}_o \phi_o(k_x - 9\pi^2) - \pi^6 \bar{v}_o \\ \phi_o \left(\bar{k}_t - \pi^2 \right) \left(\bar{k}_t - 9\pi^2 \right) &= \\ = \beta^2 \left\{ \bar{y}_o \left[A_1 \left(\bar{k}_t - 9\pi^2 \right) + A_3 \left(\bar{k}_t - \pi^2 \right) \right] + \bar{x}_o \left[A_2 \left(\bar{k}_t - 9\pi^2 \right) - A_4 \left(\bar{k}_t - \pi^2 \right) \right] \right\} \end{aligned} \quad (17)$$

Setting

$$\rho_x = \frac{C_w}{I_x \ell^2}, \quad \rho_y = \frac{C_w}{I_y \ell^2}, \quad \mu = \frac{I_o}{A \ell^2}, \quad \lambda = \frac{GJ \ell^2}{EC_w} \quad (18)$$

eqs. (17) can be transformed as

$$\begin{aligned} \bar{u}_o(\beta^2 \rho_y - \pi^2)(\beta^2 \rho_y - 9\pi^2) + \pi^6 \bar{u}_o &= -\beta^2 \bar{\rho}_y \bar{y}_o (\beta^2 \rho_y - 9\pi^2) \phi_o \\ (\beta^2 \rho_x - \pi^2)(\beta^2 \rho_x - 9\pi^2) + \pi^6 \bar{v}_o &= 0 \\ \phi_o(\mu \beta^2 - \lambda - \pi^2)(\mu \beta^2 - \lambda - 9\pi^2) &= \\ = \beta^2 \left\{ \bar{y}_o [A_1(\mu \beta^2 - \lambda - 9\pi^2) + A_3(\mu \beta^2 - \lambda - \pi^2)] + \bar{x}_o [A_2(\mu \beta^2 - \lambda - 9\pi^2) - A_4(\mu \beta^2 - \lambda - \pi^2)] \right\} \end{aligned} \quad (19)$$

With the aid of this system one can determine numerically, for each value of the dimensionless load β^2 , the corresponding values of \bar{v}_o , \bar{u}_o , ϕ_o and establish the respective equilibrium paths. It is evident that the trivial solution $\bar{v}_o = 0$, $\bar{u}_o = 0$, $\phi_o = 0$, which represents the fundamental equilibrium paths, satisfies eqs. (19). The intersection of the fundamental path with the non-linear postbuckling path, related with eqs. (19), corresponds to the critical bifurcation state.

4. APPLICATION TO ANGLE CROSS-SECTIONS

(a) Unequal leg angles

The analysis presented above will be applied to the case of a pin-ended bar with an unequal leg angle cross-section of uniform thickness t (Fig. 2) in which x , y are the principal axes. Assuming $b_1 < b_2$ and $t \ll b_1$ eq. (6) can be written, after some elaboration, in the form:

$$\begin{aligned} \mu \rho_x \rho_y \frac{I_c}{I_o} \beta^6 + \pi^2 [\rho_y \bar{y}_o + \rho_x \bar{x}_o - \mu \pi^2 (\rho_x + \rho_y) - \rho_x \rho_y (\pi^2 + \nu)] \beta^4 + \\ + \pi^2 [\mu \pi^2 + (\pi^2 + \nu)(\rho_x + \rho_y)] \beta^2 + \pi^4 (\pi^2 + \nu) = 0 \end{aligned} \quad (20)$$

where $I_c = I_x + I_y$.

The coordinates of the shear center are given by the relations:

$$\bar{x}_0 = \bar{b}_1 \frac{\bar{b}_2 \sin \omega + \cos \omega}{2(1 + \bar{b}_2)}, \quad \bar{y}_0 = \bar{b}_1 \frac{\bar{b}_2 \cos \omega + \sin \omega}{2(1 + \bar{b}_2)} \quad (21)$$

and (Fig. 2)

$$\tan 2\omega = \frac{6\bar{b}_2}{(\bar{b}_2 - 1)(1 + 4\bar{b}_2 + \bar{b}_2^2)} \quad (22)$$

where $\bar{b}_1 = b_1/l$, $\bar{b}_2 = b_2/l$.

The postbuckling equilibrium paths can be established using eqs. (19).

In Fig. 3 the variation of the dimensionless critical load β^2 versus \bar{b}_1 is presented for steel cross sections ($G/E = 2.6$), various values of \bar{b}_2 and $\bar{t} = 0.05, 0.10$ ($\bar{t} = t/l$).

In Fig.4 the variation of the dimensionless loads \bar{P}_y and \bar{P}_t ($\bar{P}_y = P_y/P$, $\bar{P}_t = P_t/P$) against \bar{b}_1 is shown for two values of the dimensionless thickness \bar{t} .

In Fig. 5 an example of a postbuckling equilibrium path (β^2 vs. \bar{v}_0) is established using eqs. (19), for characteristic values of \bar{b}_1, \bar{b}_2, t .

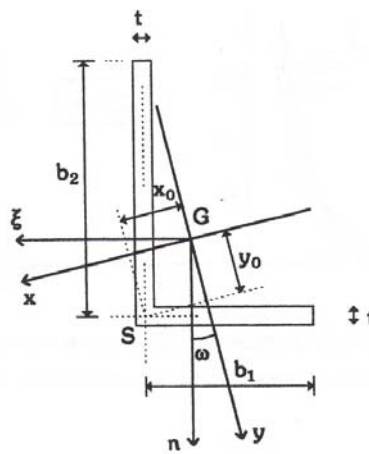


Fig. 2. Unequal-leg angle cross-section. Geometrical data.

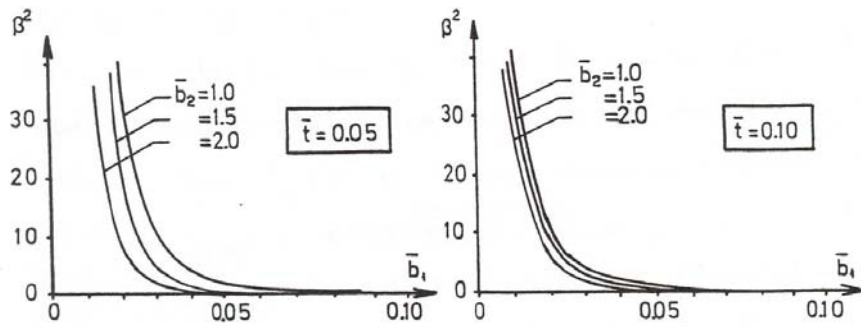


Fig. 3. Variation of the dimensionless instability load β^2 vs \bar{b}_1 for a bar with an unequal leg angle cross-section and various values of \bar{b}_2 and \bar{t} .

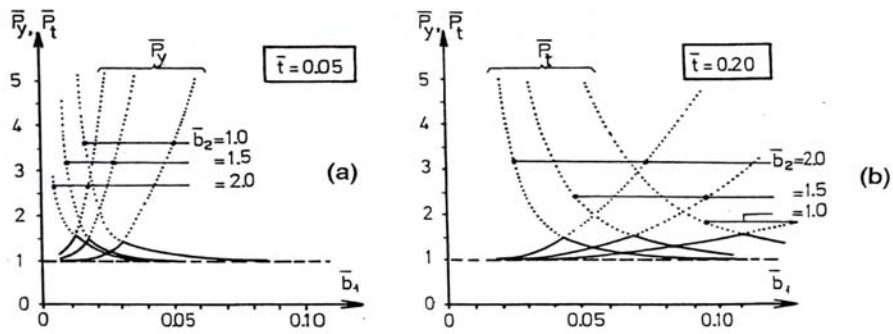


Fig. 4. Variation of \bar{P}_y and \bar{P}_t against \bar{b}_1 for a bar with an unequal leg angle cross-section and various values of \bar{b}_2 and \bar{t} .

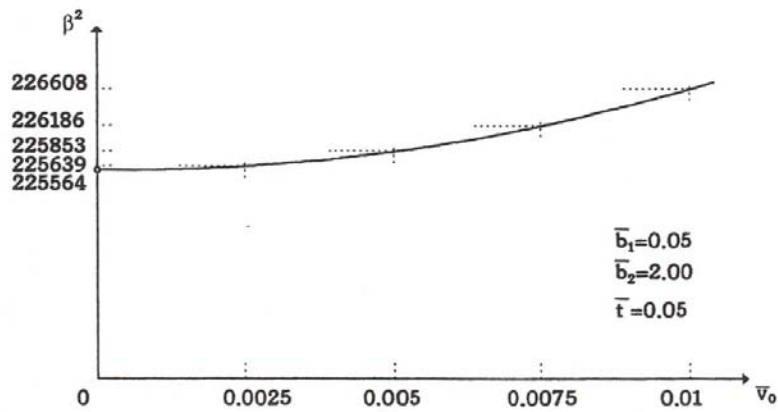


Fig. 5. Postbuckling equilibrium path for a bar with unequal-leg angle cross-section under centrally applied axial load

From the above plots the following remarks can be stated:

- (a) the critical instability load P (associated with simultaneous bending and torsion), is up to 1.6 times smaller than the smaller of P_y and P_t .
- (b) for thick cross-sections ($\bar{t} = 0.20$) and for slender bars ($\bar{b}_1 < 0.02$) the critical load of flexural-torsional buckling, practically coincides with the critical (Euler) buckling load.
- (c) for thick cross-sections ($\bar{t} = 0.20$) and bars with small slenderness ratio, P practically coincides with the critical load of torsional buckling for $\bar{b}_1 > 0.08$ (when $\bar{b}_2 = 2.00$), for $\bar{b}_1 > 0.11$ (when $\bar{b}_2 = 1.50$), and for $\bar{b}_1 > 0.15$ (when $\bar{b}_2 = 1.00$).
- (d) for thin cross-sections ($\bar{t} = 0.05$) the above coincidence is observed when $\bar{b}_1 > 0.05$ (for $\bar{b}_2 \geq 1.5$) and when $\bar{b}_1 > 0.08$ (for $\bar{b}_2 = 1.00$).
- (e) the critical bifurcation state is related to a stable and symmetric branching point. The bar develops postbuckling strength, therefore is not sensitive to initial imperfections. Nevertheless the postbuckling paths are very shallow, so the margin of the postbuckling strength is limited.

(b) Equal leg angles

For the specific case of equal leg angles ($b_1=b_2$) the variation of the dimensionless critical stress σ_{cr}/E of lateral torsional buckling (according to a simultaneous flexural and torsional configuration) vs the thickness \bar{t} for two different values of the width \bar{b} is presented in Fig.6. The above critical stress is compared with the level of the corresponding critical stress of flexural buckling (σ_x/E). From these diagrams one could conclude that the buckling according to a simultaneous flexural and torsional configuration can be critical for short elements and steel qualities with a high value of the yield stress (high strength steels). For instance in the case of $\bar{b} = 0.10$ (Fig. 6b) the flexural-torsional buckling is critical (compared with pure flexural or torsional buckling) for $\bar{t} < 0.11$ i.e. for the currently used area of thickness. For more slender bars the flexural-torsional mode of buckling is critical for relatively small values of the thickness (Fig. 6a), which are not of practical interest because local buckling phenomena govern the behaviour and the strength of the bars.

In Fig. 7 the postbuckling equilibrium path (β^2 vs \bar{u}_o) for equal-leg angle with $\bar{b}=0.10$ and $\bar{t}=0.10$ is presented. The remark concerning the shallowness of this path is also valid.

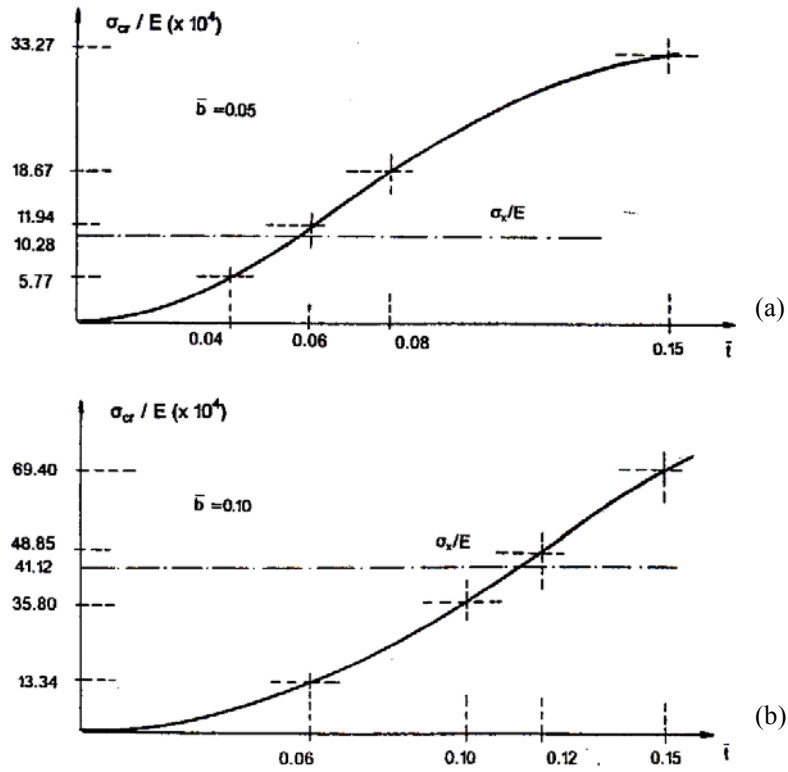


Fig. 6. Dimensionless axial critical stress σ_{cr}/E of lateral-torsional buckling vs thickness \bar{t} of the equal-leg angle cross section for various values of the width \bar{b} of the angle ($\bar{b}=0.05, 0.10$)

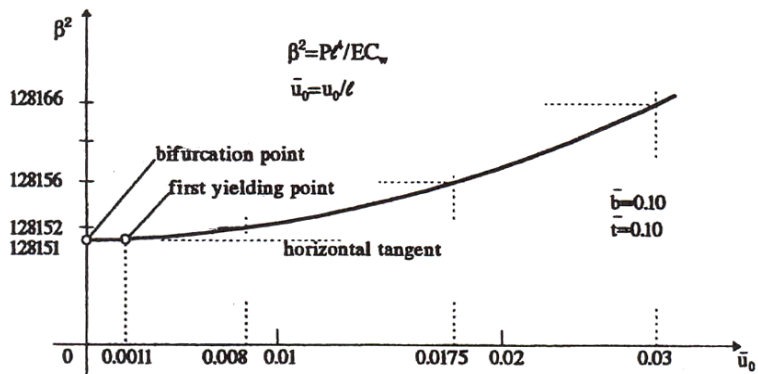


Fig. 7. Initial postbuckling path β^2 versus \bar{u}_0 of a simply supported bar with equal leg cross-section, under simultaneous bending and torsion due to axial load. First yielding point

5. ELASTIC LIMIT STATE

Eqs. (19) are valid provided that the bar behaves, in the postbuckling range of behaviour, elastically. The present section deals with the onset of first yielding occurring at the initial postbuckling path.

Clearly, first yielding occurs when the maximum normal stress in the cross-section becomes equal to the yield stress of the material of the bar. This stress is given by

$$\sigma_{\max} = \sigma_y = \sigma_o + \sigma_{by} + \sigma_w \tag{23}$$

where $\sigma_o = P/A$ is the uniform stress due to axial compression; $\sigma_{by} = M/Z_y = Pu_o/Z_y$ is the maximum bending stress (Z_y the elastic section modulus about the y axis) and σ_w is the maximum normal stress due to warping.

The normal warping stress σ_w in Eq. (23) is defined as [12]

$$\sigma_w(z) = E\phi''(z)(w_1 - \bar{w}_1) \tag{24}$$

where

$$w_1 = \int_0^s r_s ds + nr_n \tag{25}$$

The distances r_s and r_n in Eq. (25) are shown in Fig. 8, representing an open thin-walled cross-section, where S is the shear center and A (being the intersection of the axes s and n) is an arbitrary point of the mean line (of the cross-section) of length s , \bar{w}_1 is the mean value of w_1 and n the distance from the mean line to any point on the cross-section. For thin-walled open sections the maximum value of n is $t/2$.

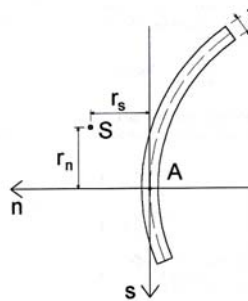


Fig. 8. Distances r_s and r_n related to the warping constant of a thin walled cross-section

Applying the above in the case of an equal-leg angle we can, after some elaboration, obtain

$$\begin{aligned} \sigma_o &= P/A = \frac{1}{36} E t^{-2} b^{-4} \beta^2, \\ \sigma_{by} &= Pu_o/Z_y = \frac{\sqrt{2}}{12} E t^{-2} b^{-3} u_o \beta^2. \end{aligned} \tag{26}$$

Concerning the normal stress due to warping for the considered cross section $r_s = 0$, $\bar{w}_1 = 0$ and therefore

$$\sigma_w(z) = E\phi''(z)w_1 = E\phi''(z)nr_n = E\phi''(z)bt/2. \quad (27)$$

At the mid-height of the bar, according to eqs. (4), $\phi''(1/2) = \phi_0\pi^2/1^2$. Hence the maximum normal stress due to warping is

$$\sigma_w = \frac{1}{2}btE\phi_0\frac{\pi^2}{1^2} = \frac{\pi^2}{2}Etb\phi_0. \quad (28)$$

Using eqs. (26) and (28), eq. (23), the condition corresponding to the first yielding of the bar, can be finally expressed as

$$\frac{Etb}{\sigma_y} \frac{1}{2} \left\{ \frac{1}{18}tb(b+3\sqrt{2}u_0)\beta^2 + \pi^2\phi_0 \right\} = 1. \quad (29)$$

With the aid of the above equation (29), in conjunction with eqs. (19), the level of the external loading β^2 , related to the onset of first yielding of the bar can be determined. Using the geometrical data of the cross section corresponding to Fig. 7 the first yielding point is shown on the postbuckling equilibrium path (Fig.7).

As one can remark the first yielding point is very near to the critical bifurcational point. Therefore, as it is already sited, eqs. (19) correspond only to the initial part of the postbuckling path and are appropriate to determine the nature of this bifurcation.

6. APPLICATION TO OTHER CASES OF CROSS-SECTIONS

(a) Channel rolled cross-section

Applying the linear analysis, previously presented, in the case of a channel rolled cross-section the variation of the dimensionless critical stress of flexural - torsional buckling σ_{cr}/E as a function of: the dimensionless thickness $\bar{t} = t/b$ (b the width of the flanges), the width $\bar{b} = b/h$ (h the height of the cross-section) and the height $\bar{h} = h/\ell$ is presented in plots (Fig.9). In the plots the comparison with the critical load of flexural buckling (straight lines) is also shown.

Then for the case of a channel cross-section, $\bar{x}_0 = 0$, the system of eqs. (19) for establishing the postbuckling equilibrium path is simplified. Figure 10 shows such a path (β^2 vs ϕ_0) for a channel with $\bar{h} = 0.05$, $\bar{b} = 0.50$ and $\bar{t} = 0.025$. In the same plot the point E, corresponding to the elastic limit state, is placed on the above equilibrium path with the aid of eq. (23).

(a) Monosymmetric I - cross-section

This example is related to the simply supported beam with the monosymmetric cross-section shown in Fig. 11a. The cross section is associated with the following geometrical data and elastic constants:

$$\begin{aligned} I_x &= 72808 \text{ cm}^4, I_y = 5076 \text{ cm}^4, A = 165 \text{ cm}^2, x_0 = 0, y_0 = 15.49 \text{ cm}, I_0 = 117474 \text{ cm}^4, \\ J &= 178.5 \text{ cm}^4, C_w = 1352000 \text{ cm}^6, E = 21000 \text{ kN/cm}^2, G = 8077 \text{ kN/cm}^2, \\ \rho_x &= 1.5 \cdot 10^{-5}, \rho_y = 2.1617 \cdot 10^{-4}, \mu = 5.7784 \cdot 10^{-4}, \lambda = 62.565 \end{aligned}$$

From the linear analysis it follows that $P_{cr} = 739.17$ kN and for the dimensionless critical load $\beta^2 = 39522$. With the aid of eqs. (19) the postbuckling equilibrium path (β^2 vs \bar{u}_0), shown in Fig. 11b, is established.

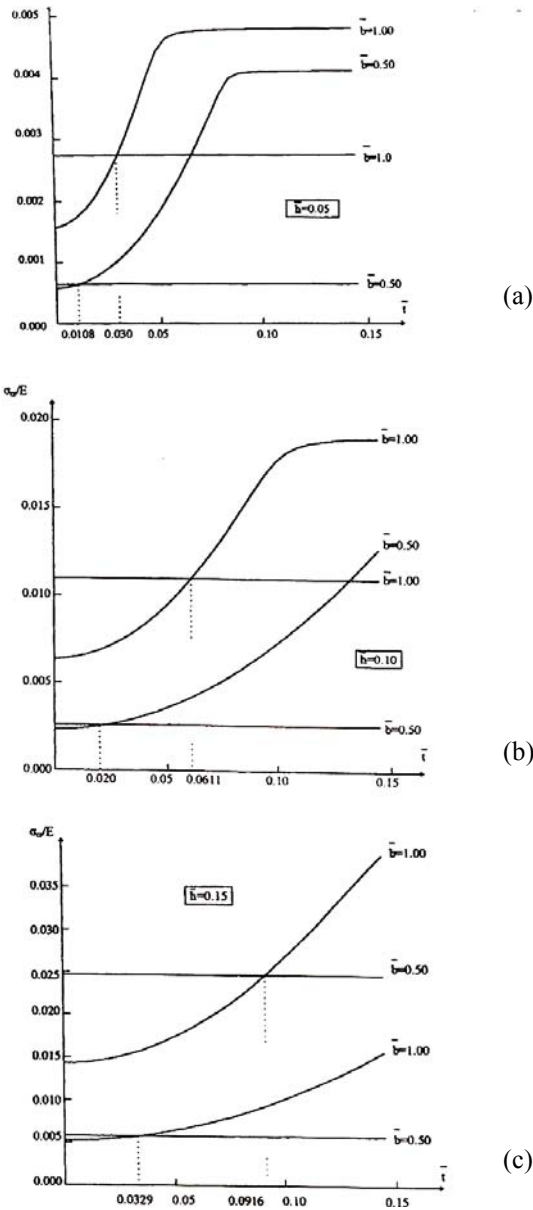


Fig. 9. Dimensionless axial critical stress of flexural-torsional buckling vs thickness \bar{t} of the channel cross-section for various values of \bar{b} , \bar{h} . Comparison with the critical dimensionless stress of flexural buckling.

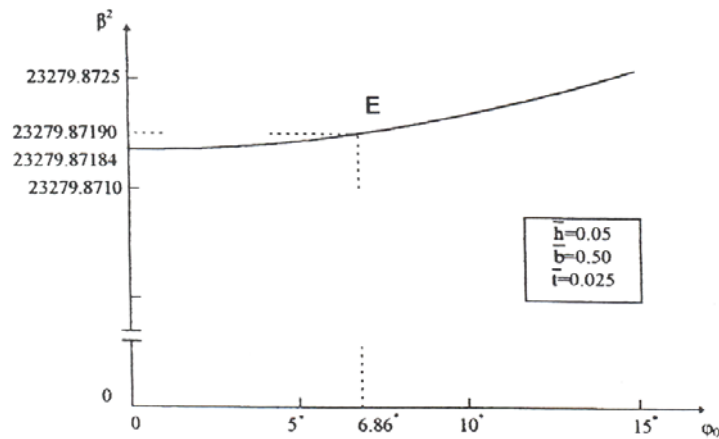


Fig. 10. Initial part of the postbuckling path (β^2 vs $\bar{\phi}_0$) of a simply supported bar with a channel cross-section, under simultaneous bending and torsion due to axial compression. First yielding point.

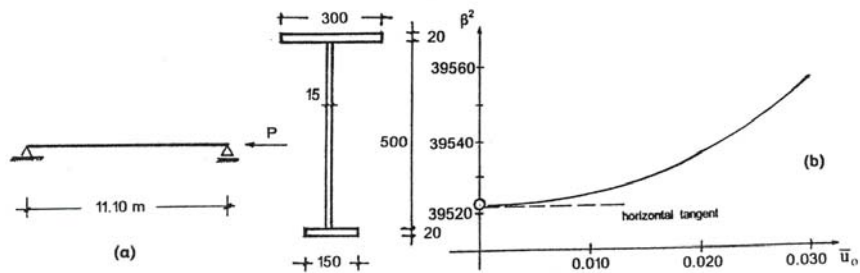


Fig. 11. Simply supported steel bar with monosymmetric I-section and initial postbuckling path β^2 vs \bar{u}_0

CONCLUSIONS

The most important conclusions of the present study are the following:

- A simple and efficient technique for establishing the initial part of the postbuckling equilibrium path is presented, for the case of axially compressed bars with open thin-walled cross-sections having one, or without, axis of symmetry.
- The critical instability state is related to a stable and symmetric bifurcation point.
- The postbuckling equilibrium paths are very shallow and therefore the postbuckling strength is very limited.
- Considering bars made of ideal elastic - ideal plastic material, their elastic limit state associated with first yielding can also be determined.
- First yielding is related to the maximum normal stress in the middle cross-section of the simply supported bar, being equal to the yield stress of the bar's material. The above maximum normal stress is determined as a function of the uniform stress due to axial compression, of the maximum bending stress and of the maxi-

mum normal stress due to warping. One should notice the importance of the normal stress due to warping, which can reach, in some cases, an appreciable percentage of the total normal stress.

- (f) Due to the shallowness of the postbuckling path first yielding takes place near to the critical state.
- (g) Areas of the geometrical data of bars with unequal-leg angle cross-section for which the critical instability load practically coincides with the critical loads of pure flexural or pure torsional buckling, are indicated.
- (i) Areas of the geometrical data of bars with channel or equal-leg angle cross-sections for which the lateral-torsional buckling configuration is critical are also presented in graphs.

REFERENCES

1. Vlassov BZ., Pieces lonques en voiles minces, Eyrolles, Paris, 1962.
2. Chen WF, Atsuta T., Theory of beam-columns, McGraw-Hill, NY, 1977.
3. Trahair NS., Flexural-torsional buckling of structures, E.N. Spon, London, 1993.
4. Woolcock ST, Trahair NS., Postbuckling behaviour of determinate beams, J. Eng. Mech. Div., ASCE 1974;100(EM2):151-71.
5. Woolcock ST, Trahair NS., Postbuckling of redundant I-beams, J. Eng. Mech. Div., ASCE 1976; 102(EM2):293-312.
6. Kounadis AN, Ioannidis GI., Lateral postbuckling analysis of beam-columns, J. Eng. Mech. Div., ASCE 1994;120(4):695-706.
7. Ioannidis GI, Kounadis AN., Lateral postbuckling analysis of monosymmetric I-beams under uniform bending, J. Constr. Steel Res. 1994;30: 1-12.
8. Ioannidis GI, Ermopoulos JH., Kounadis AN, Stability analysis of bars with asymmetric open thin walled cross-sections under eccentric axial thrust, Acta Universitatis, University of Nis, 1999.
9. Kounadis AN., Postbuckling analysis of bars with thin-walled cross-sections under simultaneous bending and torsion due to central thrust, J. Constr. Steel Res. 1998; 45:17-37.
10. Kounadis AN., An efficient and simple approximate technique for solving nonlinear initial and boundary-value problems, Comp. Mech. 1992;9:221-31.
11. Timoshenko S, Gere J., Theory of elastic stability. McGraw-Hill, NY, 1961.
12. [12] Oden JT., Mechanics of elastic structures. McGraw-Hill, NY, 1967,

ANALIZA PONAŠANJA SAVIJENIH CENTRIČNO PRITISNUTIH TANKOZIDNIH GREDA OTVORENIH POREČNIH PRESEKA

G.I. Ioannidis

U radu je analizirano ponašanje savijenih tankozidnih greda konstantnog poprečnog preseka pritnutih centralnim opterećenjem. Analiza se odnosi na slučaj kada se centar smicanja ne poklapa sa težištem poprečnog preseka, i greda gubi stabilnost u uslovima spregnutih naprezanja na savijenje i uvijanje. Putevi stabilnosti grede u savijenom stanju su određeni korišćenjem jednostavnih analitičkih tehnika koje dovode do zaključaka da su u graničnim slučajevima naponi ograničeni. Pažnja je usmerena na prvo tečenje, u slučaju da je greda načinjena od idealno elastičnog-idealno plastičnog materijala, koje se javlja u početnom delu post-kritičnog puta i pridružuje se maksimumu kombinacije normalnog napona usled aksijalne kompresije, savijanja i uvijanja. Numerički primeri su predstavljeni za različite tipove poprečnih preseka.

Ključne reči: ponašanje savijene tankozidne grede, otvoren poprečni presek, centar smicanja, centar savijanja, stabilnost, post-kritični put, idealno elastični, idealno plastični material.